Zhang, T., Lee, K.S., and Chen, Q. 2009. "A simplified approach to describe complex diffusers in displacement ventilation for CFD simulations," *Indoor Air,* 19(3), 255-267.

A simplified approach to describe complex diffusers in displacement ventilation for CFD simulations

Tengfei (Tim) Zhang[1], Kisup Lee[2], and Qingyan (Yan) Chen[2]

[1]School of Civil and Hydraulic Engineering, Dalian University of Technology (DUT), 2 Linggong Rd, Dalian 116023, China
[2]School of Mechanical Engineering, Purdue University, 585 Purdue Mall, West Lafayette, IN 47907, USA

Abstract

With the capability to improve indoor air quality while simultaneously reduce energy demand, displacement ventilation is becoming popular. However the numerical simulation of air distribution in an indoor space with displacement ventilation using computational fluid dynamics (CFD) is challenging due to the complexity of air diffuser geometry and the complicated airflow pattern generated. Typical air diffusers used for displacement ventilation systems include, but not limited to, quarter-circular-perforated, grille, floor-perforated, and swirl diffusers. None of them can be treated as a simple opening in CFD simulations because their effective area ratios are small. This investigation has developed a new, simple method to describe those diffusers by directly specifying correct jet momentum from the diffusers while adjusting the airflow rate by changing the effective areas. This is done by setting some CFD cells for a diffuser with a certain momentum, while other cells are randomly blocked. By implementing this method into a commercial CFD program, this study used the method to simulate air distributions in an office and a workshop with those diffusers under cooling or heating conditions. The distributions of air velocity, temperature, and airborne contaminant concentration are in good agreement with the corresponding experimental data obtained from an environmental chamber.

Practical implications

This paper presents a simplified method for description of complex diffusers in CFD simulation of displacement ventilation at high computational efficiency. It can be used to assist design and analysis of air distribution for displacement ventilation as well as other types of ventilation with complex diffusers.

Introduction

Numerous studies have revealed that displacement ventilation can provide better indoor air quality than the traditional mixing ventilation systems (Chen and Glicksman, 2003; Bauman and Daly, 2003). Some studies (Hu et al., 1999; Lau and Chen, 2006; Wachenfeldt et al., 2007) have also shown that displacement ventilation has higher energy efficiency that could lead to reduction of energy demand by the heating, ventilating and air-conditioning (HVAC) systems. Thus, displacement ventilation has gained great popularity in building industry since

it was first used in Europe in the 1970s. Due to the wide use of displacement ventilation, ASHRAE (the American Society of Heating, Refrigerating and Air-Conditioning Engineers; Chen and Glicksman, 2003; Baumann and Daly, 2003) and REHVA (the Federation of European Heating and Air-Conditioning Associations; 2002) have developed respectively design guidelines of displacement ventilation for designers.

In order to assess the performance of displacement ventilation, both experimental test and numerical simulation by computational fluid dynamics (CFD) modeling have been widely used (Riffat et al., 2004). CFD simulation of displacement ventilation can provide very detailed information of the system performance at a much lower cost compared with experimental tests. As identified in many studies (Huo et al., 2000; Sun and Smith, 2005; Einberg et al., 2005; Srebric and Chen, 2000, 2002), correct description of air diffusers in CFD plays a critical role in accurate simulation of air distribution in an indoor space because the flow characteristics from the diffusers usually dominate airflow in an indoor space. However, the appropriate description of air diffusers used in displacement ventilation is very difficult in CFD. Most commonly-used diffusers in displacement ventilation have very complicated geometry, such as a quarter-circular-perforated, grille, floor-perforated and swirl diffusers as shown in Figure 1. The major obstacle for CFD simulation lies in the fact that such a diffuser has a relatively small size as compared to that of an indoor space but usually has stronger momentum (Srebric and Chen, 2000, 2002). It is not feasible to use tens of thousands of grid cells for calculating indoor airflow from the diffuser. How to use a few grid cells to accurately simulate such complex diffusers is a bottleneck for CFD analysis of a ventilated space with displacement ventilation (Srebric and Chen, 2002). Therefore, this paper details our effort to develop a new simple method to describe those diffusers of displacement ventilation systems for CFD simulations.

A brief review of diffuser description in CFD simulations

Many attempts have been carried out on CFD simulation of diffusers. Available approaches can be generally categorized into the direct description, simplified geometry, box, momentum, and prescribed velocity methods.

The direct description method draws the actual geometry of a complex diffuser without using approximations. Thus the simulation domain is usually required to extend to include a section of duct outside of the diffuser, where the determination of boundary conditions is easier. Hu (2003) used this method to simulate a swirl ceiling diffuser. Xu and Niu (2003) did similar work but for a floor supply diffuser. Since an actual diffuser may have complex geometries such as louvers, vanes, perforated holes, or curving surfaces, the drawing of complicated geometries and the associated mesh generation in CFD may not be easy. Some researchers (Fontaine et al., 2005) pointed out that the direct description method may impose difficulties in achieving numerical convergence because of huge difference in mesh size for the diffuser and the indoor space. On one hand, due to the relatively small size of a diffuser compared with an indoor space and often the complicated airflow pattern from the diffuser, the meshes employed for the diffuser should be sufficiently fine to capture the flow characteristics. On

the other hand, to minimize computational burden, relatively coarse meshes should be used in the rest regions of the space. Even with improvement of computing speed and capacity at present, the computational demand is not trivial with ultra fine meshes for diffusers. Therefore, the direct description method has not gained popularity.

Instead of drawing the actual geometry of a diffuser, the simplified geometry method approximates the openings to simplified alternatives with the same effective areas. This method is also called the basic model method (Heikkinen, 1991) or the conventional method (Huo et al., 2000). Heikkinen (1991) used this method to simulate a complex diffuser composed of 84 round nozzles by approximating them into slot openings. Zhao et al. (2003) also used this method to simulate a wall-mounted perforated, a grille, and a square-ceiling diffuser, respectively, where the perforated and grille diffusers were approximated into one opening while the square ceiling diffuser was simplified into nine openings. Sun and Smith (2005) simulated a square cone diffuser by simplifying it into nine pieces, where the discharge velocities and directions at each piece were determined by a separate simulation just for a volumetric region including the end of duct, diffuser and a small part of the room surrounding the diffuser. Djunaedy and Cheong (2002) proposed five schemes to model a four-way ceiling diffuser by changing the shapes and positions of openings to form the effective discharge areas. Bin and Sekhar (2007) also used the scheme recommended by Djunaedy and Cheong (2002) to study a ceiling diffuser. Although the above researchers have achieved considerably reasonable results, this approach has poor performance for non-isothermal flows (Chen and Moser, 1991) especially for diffusers with small effective area ratios (Emvin and Davidson, 1996), and even can lead to wrong results sometimes (Kurabuchi et al., 1989). In addition, it is hard to reach an agreement on how to simplify diffuser geometry with this approach. Therefore, in spite of simplicity of the simplified geometry method, the success is not assured.

The box method does not specify flow and thermal boundary conditions on a diffuser. Instead, it determines flow and thermal conditions on imaginary surfaces of a box surrounding the diffuser in an indoor space (Nielsen, 1997). Thus, the role of a diffuser in a room is transferred to the defined box. Since the flow and thermal conditions on the imaginary surfaces of the box are unknown, they are measured to make CFD simulation viable. Kotani et al. (2002) used the box method to simulate a multi-cone ceiling diffuser and concluded the validity of this method after comparing the results with the experimental data. Emvin and Davidson (1996) also obtained similar conclusions. It should point out that the determination of thermal and flow conditions on the imaginary surfaces of the box is not easy. Furthermore, some researchers (Xu and Niu, 2003) found that the box method is not suitable for flows at low Reynolds numbers, which are usually the cases in displacement ventilation because the jet flow decays rapidly. In addition, the criteria to determine the box size seems contradictory, since on one hand the box size should be large enough to make the box boundary lie in the fully developed regions of the jets, and on the other hand the box should be as small as possible to minimize the impact of room conditions to the jets (Srebric and Chen, 2000).

The challenges in simulating a diffuser by CFD do not only lie in the complexity of the diffuser geometry but also in how to specify correctly flow conditions to satisfy both the mass

and moment equations. The simplification of a diffuser into one opening in the same size of the diffuser leads to problems since the effective area ratio is usually small. For example, if a diffuser is approximated into one opening with correct mass flow rate, the induction momentum by the jet will be much smaller than the reality. The momentum method (Chen and Moser, 1991) was thus proposed to remedy the problem by specifying different velocities for the continuity and momentum equations on a diffuser. The momentum method is also called as the momentum method at air supply devices (Srebric and Chen, 2002). Chen et al. (1991) and Jiang et al. (1992) applied the momentum method to simulate complex diffusers for mixing and displacement ventilations. Srebric and Chen (2002) compared the box method and the momentum method in simulating eight typical diffusers and concluded that the momentum method should be used whenever possible due to its simplicity. Since the velocity used for the continuity equation is different from that for the momentum equation, some researchers (Xu and Niu, 2003; Kurabuchi et al., 1989) claimed that the momentum is not conserved. Furthermore, not all the commercial CFD software can use the method for a diffuser.

The prescribed velocity method uses a simple opening that has the same size as a diffuser. By using correct mass flow rate for the diffuser the air velocity will be smaller than that from the actual opening because the effective area ratio is smaller than one for most diffusers. The method compensates for momentum by prescribing the actual, higher air velocity profile in a small distance at the diffuser front. The profile could be measurement data or be determined by using jet formulae. This method is also called as the momentum method in front of air supply devices (Srebric and Chen, 2002). Theoretically, there is no substantial difference between the momentum method and the prescribed velocity method, because both methods define the actual mass flow rate at the diffuser opening and then compensate for the momentum loss. The momentum method compensates at the diffuser surface while the prescribed velocity method does it at a distance in front of the diffuser. Koskela (2004) used the prescribed velocity method to simulate a nozzle diffuser. Huo et al. (2000) used jet formulae for the prescribed velocity method to simulate a ceiling supply diffuser. Einberg et al. (2005) used the method to simulate an industrial air diffuser composed by a combination of a circular displacement diffuser and a multi-cone diffuser at the bottom part. The displacement diffuser was used for air discharge at low velocities, while the multi-cone diffuser allowed for high velocity discharge. Luo and Roux (2004) and Luo et al. (2004) also applied this method to add extra momentum to simulate nozzle arrays. Fontaine et al (2005) compared the direct description method, the simplified geometry method, and the prescribed velocity method for a circular ceiling diffuser and concluded that the prescribed velocity method performed best. Due to lack of general formulae in predicting jet flow, the prescribed velocity method often requires the velocity profile to be measured. Furthermore, the method may alter the actual flow conditions near a diffuser with the additional momentum artificially added into the jet discharge region.

The above review reveals that among the five available methods in describing air diffusers for CFD simulations, the direct description method requires very fine meshes to describe the diffuser so that the computing cost is high and it may have numerical convergence problem.

The simplified geometry method would work for some diffusers but the results are often not accurate. The box and prescribed velocity methods can only be applied with measured flow data. The momentum method is not conserved and is only available for some special CFD software. Therefore, this investigation tries to remedy the problems.

A new simplified method for describing a complex diffuser for CFD simulations

CFD simulation of air diffusers needs to specify correct flow, thermal and species conditions on them, especially accurate flow conditions to assure correct momentum and mass flow rate. The discharge velocity for the diffusers shown in Figure 1 is normal to the diffuser surfaces except that for the swirl diffuser where both axial and tangential velocity components co-exist. Actual discharge velocity should be specified as CFD boundary conditions for the diffusers. However, the mass flow rates will be over specified if these diffusers are simply approximated into full openings without changing the size. The simplification of the diffusers into several openings with reduced size using the simplified geometry method may not work either, since it is hard to distribute these openings at appropriate positions to accurately represent the actual flow conditions.

This paper proposed to specify flow conditions on CFD cells of simplified diffuser geometry. The new method assigns the actual velocities on a certain ratio of CFD cells while the other cells are randomly blocked. According to the mass conservation principle, the ratio to be treated as openings should be equal to the effective area ratio of the diffuser. Figure 2 shows the randomly open and blocked cells for the four diffusers in displacement ventilation. This method uses the following random mathematical function to determine if a CFD cell is open,

$$random(i) \geq \varepsilon \tag{1}$$

where $random(i)$ is a mathematical function to generate a random float number evenly distributed between 0 and 1, i is an integral seed and is also the CFD cell index ranging from 1 to N (the maximum CFD cell number), ε is the effective area ratio of the diffuser. If N is not too small, the percentage of open cells should be close to the diffuser effective area ratio. It is important to ensure that the CFD cell number for a diffuser, N, is large enough to obtain grid-independent results. The grid-independence check shall guarantee major flow features have been captured and more crucially the ratio of open cells is equal to ε. Otherwise, a larger N is required.

The most important boundary conditions to be determined on a diffuser in CFD simulation is the discharge air velocity. The velocity can be determined by the following formula if the flow is uniform on the diffuser surfaces,

$$U_0 = \frac{\dot{m}}{\rho A_0} \tag{2}$$

where, U_0 is the normal discharge velocity, $\dot{m}$ is the mass flow rate, ρ is the air density, and A_0 is the diffuser effective area. If any of airflow rate, discharge angles, diffuser geometry parameters and turbulence intensity are unknown from design, they should be determined by experimental measurements. When a diffuser discharges flow in different directions, the diffuser conditions have to be measured and modeled with at least two velocity components, such as a swirl diffuser. For a very complicated diffuser, this method shall be used after dividing the diffuser into several simple pieces.

Since commercial CFD software such as FLUENT (http://www.fluent.com) provides very friendly user interface for programming, the specification of discharge velocity and open/blocked CFD cells are relatively easy.

Case description

In order to test the new method for diffuser description, this paper has investigated four indoor spaces with displacement ventilation as shown in Figure 3. An environmental chamber that was 4.92 m in length, 4.32 m in width, and 2.42 m in height was used to simulate these four cases. Detailed experimental measurements were conducted in the chamber to obtain quality data for validating the new method. The diffusers used in these spaces were the same as those shown in Figs. 1 and 2. The diffusers supplied cool/warm air to the indoor spaces.

In cases (a) and (b), the office had a file cabinet in one corner of the room and two tables and desk computers in the other two corners. Six fluorescent lamps were mounted at the ceiling to provide illumination for the office. Two occupants simulated by box-shaped manikins were seated sedentarily in front of the tables. Only one contaminant source mimicked by a tracer gas, sulfur hexafluoride (SF_6), was introduced to the head level of an occupant. Both cases were for cooling.

Case (c) was a workshop with four persons doing assembling work inside. Four heated boxes on the tables were used to mimic the heat generation from the assemble lines. Again, a contaminant source was introduced to the head level of one seated person and the case was for cooling.

Case (d) was an office with three chilled windows on one side wall that mimicked a winter scenario. Warm air was supplied through the two swirl diffuser to keep a thermally comfortable condition.

Table 1 shows the boundary conditions for flow, heat and species in these four indoor spaces. The two swirl diffusers supplied warm air at different temperatures in the experiment.

The experiment measured the distributions of air velocity, temperature and SF_6 concentration. Many hot sphere anemometers were mounted at different heights in the chamber to measure

the vertical profiles of air velocity and temperature at nine different locations as shown in Figure 4. The accuracy of the anemometers for velocity was 0.02 m/s with 1% error, and for air temperature was 0.2 ^{o}C with 1% error. Due to the convection generated from the sensors, there were uncertainties when the velocity was lower than 0.20 m/s. Two more accurate ultrasonic anemometers were applied to measure the discharge air velocities from the diffusers. The accuracy of the ultrasonic anemometers for velocity components was 0.005 m/s with 1% error. A photo acoustic, multi-gas monitor with a multi-point sampler was used to measure SF_6 concentrations. The accuracy of the tracer-gas measurements was 0.01 ppm and the repeatability was 1% of the measured values.

The CFD solved the following Reynolds-averaged Navier-Stokes (RANS) equations,

$$\frac{\partial(\rho\phi)}{\partial t} + (\rho\vec{u}\cdot\vec{\nabla}\phi) = \Gamma_{\phi}\vec{\nabla}^{2}\phi + S_{\phi} \qquad (3)$$

where ϕ is a dummy scalar variable, t is time, $\vec{u}$ is the velocity vector, Γ_{ϕ} is the effective diffusion coefficient, and S_{ϕ} is the source term. The above equation can represent the continuity, momentum, energy, contaminant concentration, turbulent kinetic energy and its dissipation rate equations by assigning different values to the dummy variable ϕ. The Re-Normalization Group (RNG) k-ε model (Yakhot et al., 1992) was used due to its stable performance (Zhang et al., 2007). The differential equations were solved with the finite volume method by dividing the domain into many spatial cells with the SIMPLE algorithm.

This study used GAMBIT to build the geometry domain of the four cases and generated the cells for CFD simulation. Both combined structured (hexahedral grids) and unstructured (tetrahedral grids) meshes were created in all cases using the Tet/Hybrid scheme with Hex core. Grid distance near the diffuser is around 0.005 m and then gradually changes into 0.08 m when approaches the core region of the domain. Slight differences exist among the four cases. The cell numbers for case (a), (b), (c) and (d) are 247 k, 226 k, 383 k, 282 k, respectively.

Table 1 lists the total heat release rate from all heat sources and the average temperature for the heated surfaces. The CFD modeling did not include radiation in this paper. Since air is almost transparent, it does not absorb radiative rays. But radiation heat transfer did occur between solid wall surfaces and thus can affect air temperature distribution through solid walls. Hence, convective heat was used as input in CFD modeling and the ratio of convective and radiative heat for heat sources was estimated according to ASHRAE Handbook - Fundamentals (ASHRAE, 2005). It was possible by directly specifying the measured temperature conditions for these heat sources. However, the surface temperature was not very uniform. Our experience shows that it is better to specify convective heat transfer fluxes.

Results and discussions

The office with a corner-mounted, quarter-circular perforated diffuser

The discharge airflow from the quarter-circular-perforated diffuser was quite uniform. The measured average discharge velocity from the diffuser was 0.28 m/s and the total volumetric flow rate was 0.065 m^3/s. According to the diffuser effective area ratio, around one third of CFD cells were blocked randomly to employ the above velocity and volumetric flow rate on the diffuser as shown in Figure 2a. The random function method was only called before the CFD iteration to set inlet boundary conditions and then they were kept unchanged until reaching a converged solution.

Figure 5 shows the vertical profiles of air velocity, temperature and SF_6 concentration, where $Z = 0$ is at the floor level and $Z = 2.42$ m is at the ceiling level. Due to limited space available, this paper only presents the results at four representative positions (P3, P5, P6 and P9) as shown in Figure 4a. Air velocities were generally low (less than 0.15 m/s). The computed results were in good agreement with the measured data. The velocities at the low part of position 3, 5 and 6 were larger than the upper part caused by the jet from the diffuser. The flow path lines from Figure 6 showed clearly how the jet was discharged on the floor level. Since when the new method describing the diffuser it did not alter the geometry nor added extra momentum source, the simulated discharge jets flowed smoothly on the floor as can be seen in Figure 6. Because positions 5 and 9 were farther away from the diffuser as compared with positions 3 and 6, the jet impact to these two locations (positions 5 and 9) was much weaker so that the velocities were low at the floor level.

The computed air temperature profiles are in excellent agreement with the measured ones as shown in Figure 5b. The jet impact from the diffuser could also be reflected in the air temperature profiles. In this case, the floor was warmer than the air next to it. The air temperatures at positions 3 and 6 were slightly lower than those in positions 5 and 9.

The SF_6 concentration profiles computed by CFD are in reasonable agreement with those measured as can be seen in Figure 5c. The agreement at positions 3 and 9 was better than that at positions 5 and 6. Since position 6 was in the vicinity of the SF_6 source, the concentration at the upper part was higher. The concentration at position 9 was uniform because this location was far away from the source. Similar to air temperature stratification, the SF_6 concentration was also stratified.

The office with two floor-grille diffusers

The grille diffusers had much smaller discharge areas as compared with the quarter-circular-perforated diffuser. The flow from the two grille diffusers in this test was highly non-uniform, due to the diffuser inside structure as shown in Figure 7a. The air was supplied from the under-floor plenum to one side of the diffuser and then was sent upwards to the room by the baffler. Figure 7b shows the normal velocity at the supply surface measured

at nine positions. The flow distribution from the two grille diffusers was almost identical. The measured volumetric airflow rate was 0.077 m^3/s. The effective area ratio was 80%, thus about 20% of the CFD cells were blocked as shown in Figure 2b.

Figure 8 compares the CFD results with measured data at four representative positions (P1, P5, P7 and P9) as shown in Figure 4b. The air velocity was generally lower than 0.15 m/s except at regions close to the diffusers (such as position 7). The difference between CFD and measured air velocity was significant at 0.1 m above the floor at position 7. This is in the recirculation region of the diffuser with very high turbulence. Both the computed and measured velocities had a great uncertainty. Otherwise, the agreement between the simulated and measured air velocities is reasonably good.

Air temperature stratification can be observed in Figure 8b. The stratification at position 7 was more evident since this location was close to the diffuser that supplied cool air. The agreement was excellent between the computed and measured air temperatures.

The SF_6 concentration was also stratified as illustrated in Figure 8c. At position 1, concentration reached its peak at around Z=1.7m, which was predicted well by CFD simulation. Although position 7 was close to the diffuser, the concentrations were high at the upper part. This is because the jet throw was not able to reach the upper part of the room and thus SF_6 could stay in this region. Such could also be explained by jet flow path lines from Figure 9. The jets from the diffuser went upward a little bit and then dropped down to the floor level due to higher density of the cool air. The agreement between the computed and measured concentration profiles was reasonably good.

The workshop with four floor-perforated-panel diffusers

The workshop with the four floor-perforated-panel diffusers was slightly different from the previous two cases. The workshop had larger cooling demand and thus higher air flow rates than the office. However, the discharge velocity from the perforated panels was quite low since the total air supply area of the perforated panels was large. The normal velocity was 0.19 m/s on the panel and the volumetric flow rate was 0.12 m^3/s. The CFD simulation blocked one third of CFD cells as shown in Figure 2c according to the effective area ratio.

As shown in Figure 10a, the air velocity in the workshop was lower than 0.1 m/s at the four representative positions (P1, P3, P4, and P8 in Figure 4c) since the air was supplied to the workshop at low momentum. As mentioned previously, the omni-directional anemometers had a great uncertainty at this low velocity because the false velocity caused by convection from the heated probes was in the same order. Nevertheless, the computed velocities agreed reasonably with the measured ones.

Air temperature stratification with 20 °C at the floor and 27 °C at the ceiling in the workshop as shown in Figure 10b was stronger than that in the office. The temperature gradient was beyond the comfort criterion recommended by ASHRAE (2004). Anyway, the occupants

inside were doing assembling work and thus might tolerate a strong temperate stratification. Again, the agreement is very good between the computed and measured air temperatures.

The computed SF_6 concentration profiles are in excellent agreement with the experimental data as shown in Figure 10c. The SF_6 concentration stratification can also be observed. Higher SF_6 concentration was found in the upper part of the room (Z>1.6 m), because the weak jet throw did not mix the room air well. Figure 11 illustrates the jet flow path lines, where the jet was clearly weak. Since position 3 was in proximity of the SF_6 source, the concentration at the upper part was very high.

The office with two swirl diffusers

Swirl diffusers are probably the most complicated diffusers one normally encounters in an indoor space. A swirl diffuser discharges jets axially and tangentially. This investigation measured both the velocity components with the ultrasonic anemometers for specifying flow conditions in CFD. The flow from the two swirl diffusers was not the same. The axial and tangential velocities were 1.16 m/s and 0.67 m/s, respectively, at the diffuser near the cabinet. Whilst, the velocities were 1.98 m/s for the axial direction and 1.14 m/s for the tangential direction, respectively, at the other diffuser. According to the effective area ratio, one third of CFD cells were blocked as shown in Figure 2d to describe the two diffusers.

Figure 12 compares the CFD results with the measured data at four representative positions (P2, P5, P6 and P8 show in Figure 4d). The air velocity was low except at position 8 that was close to the diffuser. The high velocity in the middle part of position 8 can also be observed through jet path lines in Figure 13, where the jet rotated upwards and spread to its proximity. It should be noted that warm air was supplied through the swirl diffusers. The warm jet with low air density went upwards due to buoyancy. The air velocity at the floor level of positions 5 and 6 was high, due to the downward draft caused by the chilled windows. The computed air velocity profiles are similar to the measured ones.

The air temperature distribution was uniform as can be seen in Figure 12b except near floor level. The uniform distribution was caused by the well mixing from the diffusers with warm air. Since this was a heating condition with low air temperature around, the heat was transferred to all the envelope surfaces. The agreement between the computed and measured air temperature was not as good as those in the previous three cases under cooling conditions, but still acceptable for thermal comfort study.

Since the SF_6 was released from a single point, its concentration distribution was not as uniform as the air temperature as shown in Figure 12c. The calculated SF_6 concentration profiles were not in as good agreement as the air temperature with the measured data. The reason is probably due to the single point source and unstable flow that made the measurements difficult. Our experience in other studies (Yuan et al., 1999) has also concluded that it is much harder to obtain good agreement for SF_6 concentration than that for air temperature.

The comparison of computed and measured air velocity, air temperature, and SF_6 concentration shows good agreement in the above four test cases. This may conclude that the diffusers simulated by the new method proposed in this paper could give sufficiently good flow conditions for calculating room air distributions.

In addition, the investigation also tested the random feature of the proposed method and the effect of different CFD cell numbers employed for a diffuser. The results show if both mass and momentum parameters at diffuser surface were close to the actuality, their influence to air distribution in the occupied zone was very minimal. But some differences occurred within a very small region near the diffuser due to random change of open/blocked local CFD cells at different runs. Therefore the comparison between numerical simulation and measurement has indirectly proved the validity of the new method for describing the four complex diffusers used in displacement ventilation especially in occupied zones.

Conclusions

This paper proposed a new, simple method to describe complex diffusers for displacement ventilation. It randomly blocks a few CFD cells for flow according to the effective area ratio of a diffuser to satisfy both mass flow and momentum consistency from the diffuser.

Then the method was indirectly validated by applying it with CFD to investigate four commonly-used diffusers for displacement ventilation under cooling or heating conditions. The air velocity, air temperature, and contaminant concentration profiles calculated by the CFD was compared with the corresponding measurement data obtained in an environmental chamber. Our results show that the new method is capable of describing the quarter-circular-perforated, grille, floor-perforated, and swirl diffusers under good agreement in computed profiles with the measured ones. The new method is better for diffusers with large supply areas such as the quarter-circular-perforated and the floor-perforated diffusers since their discharge flows are more uniform and stable, which are also easier to model.

References

ASHRAE. (2004) *Thermal environmental conditions for human occupancy, ANSI/ASHRAE Standard 55-2004*, Atlanta, GA, ASHRAE.

ASHRAE. (2005) *ASHRAE Handbook – Fundamentals*, Atlanta: GA, ASHRAE.

Bauman, F. and Daly, A. (2003) *Underfloor air distribution (UFAD) design guide*, Atlanta, GA, ASHRAE.

Bin, Y. and Sekhar, S. (2007) Three-dimensional numerical simulation of a hybrid fresh air and recirculated air diffuser for decoupled ventilation strategy, *Build. Environ.*, **42**, 1975-1982.

Chen, Q. and Moser, A. (1991) Simulation of a multiple nozzle diffuser. In: *Proceedings of the Twelfth AIVC Conference*, Ottawa, Canada, 1991. Vol. 2, pp. 1-14.

Chen, Q., Suter, P. and Moser, A. (1991) A database for assessing indoor air flow, air quality and draught risk, *ASHRAE Trans.* **97**(2), 150-163.

Chen, Q. and Glicksman, L. (2003) *System performance evaluation and design guidelines for displacement ventilation*, Altanta, GA, ASHRAE,.

Djunaedy, E. and Cheong, K.W.D. (2002) Development of a simplified technique of modelling four-way ceiling air supply diffuser, *Build. Environ.*, **37**(4), 393-403.

Einberg, G.., Hagström, K., Mustakallio, P., Koskela, H. and Holmberg, S. (2005) CFD modelling of an industrial air diffuser - predicting velocity and temperature in the near zone, *Build. Environ.*, **40**(5), 601-615.

Emvin, P. and Davidson, L. (1996) A numerical comparision of three inlet approximations of the diffuser in case E1 Annex 20. In: *Proceedings of the 5th International Conference on Air Distributions in Rooms (RoomVent 96)*, Yokohama, Japan, 1996. Vol. 1, pp. 219-226.

Fontaine, J., Rapp, R., Koskela, H. and Niemelä, R. (2005) Evaluation of air diffuser flow modelling methods experiments and computational fluid dynamics simulations, *Build. Environ.* , **40**(3), 377-389.

Heikkinen, J. (1991) Modelling of a supply air terminal for room air flow simulation. In: *Proceedings of the 12th AIVC Conference on Air Movement and Ventilation Control within Buildings*, Ottawa, Canada, 1991. Vol. 3, pp. 213-230.

Hu, S., Chen, Q. and Glicksman, L. (1999) Comparison of energy consumption between displacement and mixing ventilation systems for different U.S. buildings and climates, *ASHRAE Trans.*, **105**, 453-464.

Hu, S. (2003) Airflow characteristics in the outlet region of a vortex room air diffuser, *Build. Environ.*, **38**(4), 553-561.

Huo, Y., Haghighat, F., Zhang, J. and Shaw, C. (2000) A systematic approach to describe the air terminal device CFD simulation for room air distribution analysis, *Build. Environ.*, **35**(6), 563-576.

Jiang, Z., Chen, Q. and Moser, A. (1992) Comparison of displacement and mixing diffusers. *Indoor Air*, **2**(3), 168-179.

Koskela, H. (2004) Momentum source model for CFD-simulation of nozzle duct air diffuser, *Energ. Build.*, **36**(10), 1011-1020.

Kotani, H., Yamanaka, T. and Momoi, Y. (2002) CFD simulation of airflow in room with multi-cone ceiling diffuser using measured velocity and turbulent parameters in large space. In: *Proceedings of the 8th International Conference on Air Distributions in Rooms (RoomVent 2002)*, Copenhagen, Denmark, 2002. pp. 117-120.

Kurabuchi, T., Fang, J.B. and Rechard A.G. (1989) *A numerical method for calculating indoor air flows using a turbulence model* , Washington, DC, US Department of Commerce, NISTIR 89-4211.

Lau, J. and Chen, Q. (2006) Energy analysis for workshops with floor-supply displacement ventilation under U.S. climates, *Energ. Build.*, **38**, 1212-1219.

Luo, S. and Roux, B. (2004) Modeling of the HESCO nozzle diffuser used in IEA Annex-20 experiment test room, *Build. Environ.*, **39**(4), 367-384.

Luo, S., Heikkinen, J. and Roux, B. (2004) Simulation of air flow in the IEA Annex 20 test room - validation of a simplified model for the nozzle diffuser in isothermal test cases, *Build. Environ.*, **39**(12), 1403-1415.

Nielsen, P.V. (1997) *The box method - a practical procedure for introduction of an air terminal device in CFD calculation*, Institute for Bygningsteknik, Aaborg University, Denmark.

REHVA(Federation of European Heating and Air-Conditioning Associations). (2002) *Displacement ventilation in non-industrial premises*, Atlanta, GA, ASHRAE.

Riffat, S., Zhao, X. and Doherty, P. (2004) Review of research into and application of chilled ceilings and displacement ventilation systems in Europe, *Int. J. Energ. Res.*, 28, 257-286.

Srebric, J. and Chen, Q. (2000) A method of test to obtain diffuser data for CFD modeling of room airflow, *ASHRAE Trans*, **107**(2), 108-116.

Srebric, J. and Chen, Q. (2002) Simplified numerical models for complex air supply diffusers, *HVAC&R Res.*, **8**(3), 277-294.

Sun, Y. and Smith, T. (2005) Air flow characteristics of a room with square cone diffusers, *Build. Environ*., 40(5), 589-600.

Wachenfeldt, B., Mysen, M. and Schild, P. (2007) Air flow rates and energy saving potential in schools with demand-controlled displacement ventilation, *Energ. Build.*, **39**, 1073-1079.

Xu, H. and Niu, J. (2003) A new method of CFD simulation of airflow characteristics of swirling floor diffusers. In: *Proceedings of the 8th International IBPSA Conference (Building Simulation 2003)*, Eindhoven, Netherlands, pp.1429-1434.

Yakhot, V., Orzag, S., Thangam, S. and Gatski, T. (1992) Development of turbulence models for shear flows by a double expansion technique, *Phys. Fluid. A*, **4**(7), 1510-1520.

Yuan, X., Chen, Q. and Glicksman, L. (1999) Measurements and computations of room airflow with displacement ventilation, *ASHRAE Trans.*, **105**(1), 340-352.

Zhang, Z., Zhang, W., Zhai, Z. and Chen, Q. (2007) Evaluation of various turbulence models in predicting air flow and turbulence in enclosed environments by CFD: part-2: comparison with experimental data from literature. *HVAC&R Res.,* **13**(6), 871-886.
Zhao, B., Li, X. and Yan, Q. (2003) A simplified system for indoor airflow simulation, *Build. Environ.*, **38**(4), 543-552.

Table 1. Boundary conditions for the displacement ventilation with four different types of diffusers

Cases (a)		(b)	(c)	(d)
Diffuser types	quarter-circular perforated	grille	perforated -panel	swirl
Air change rate per hour (ACH)	4.57	5.41	8.62	4.09
Supply air temperature	19.0 °C	20.1 °C	19.0 °C	26.9 °C / 29.9 °C
Exhaust air temperature	26.2 °C	25.4 °C	26.7 °C	25.4 °C
SF_6 concentration at the supply	0.18 ppm	0.17 ppm	0.20 ppm	0.22 ppm
SF_6 concentration at the exhaust	0.95 ppm	0.82 ppm	0.88 ppm	1.08 ppm
Sensible heat production rate by each occupant	75 W	75 W	200 W	75 W
Heat production rate by each PC or heated box	100 W	100 W	100 W	100 W
Heat production rate by each lamp	64 W	64 W	64 W	64 W

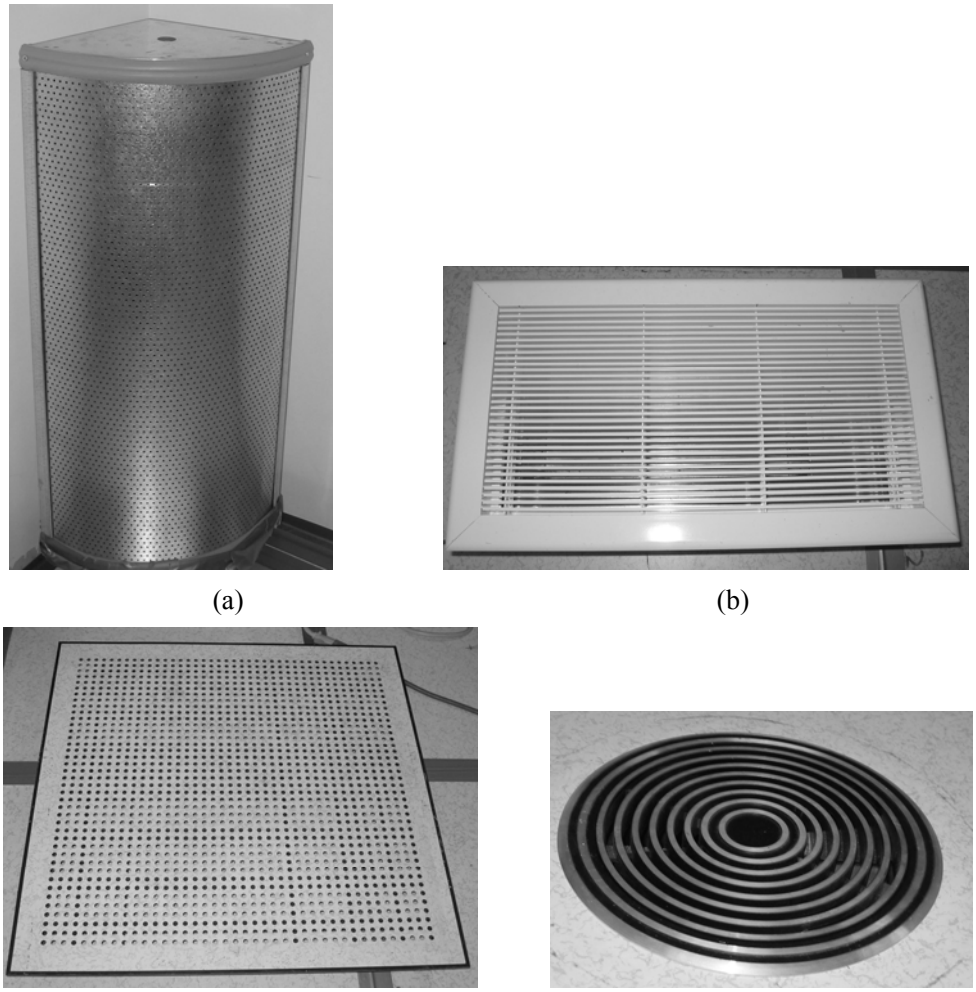

Fig. 1. Common diffusers used in displacement ventilation: (a) corner-mounted, quarter-circular perforated diffuser; (b) grille diffuser; (c) floor-perforated panel diffuser; and (d) swirl diffuser.

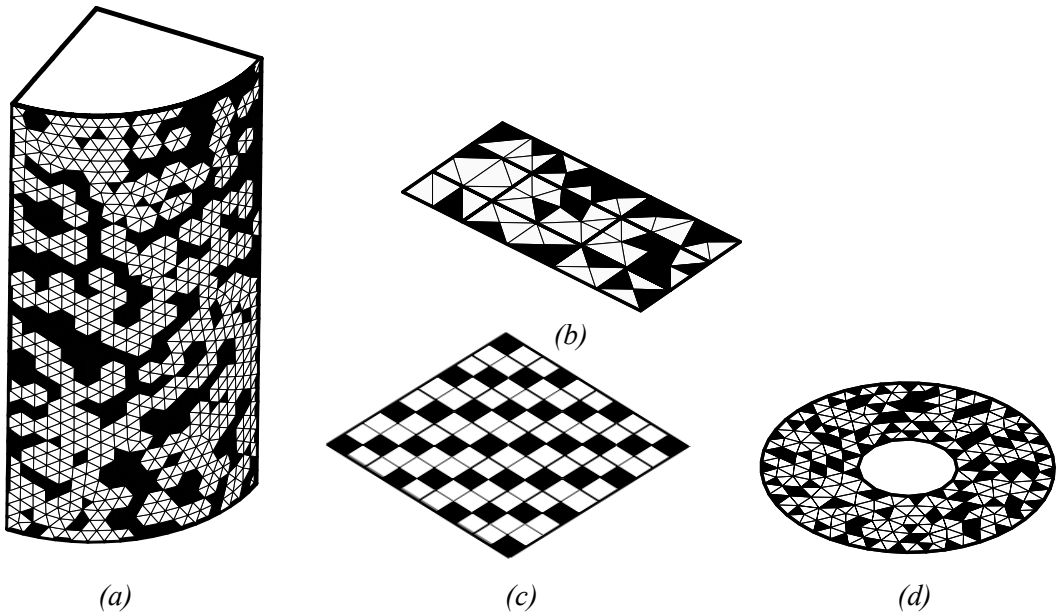

Fig. 2. Schematics of the new CFD description method of the four commonly-used diffusers where

black cells are blocked and white cells are open: (a) corner-mounted, quarter-circular perforated diffuser; (b) grille diffuser; (c) floor-perforated panel diffuser; and (d) swirl diffuser.

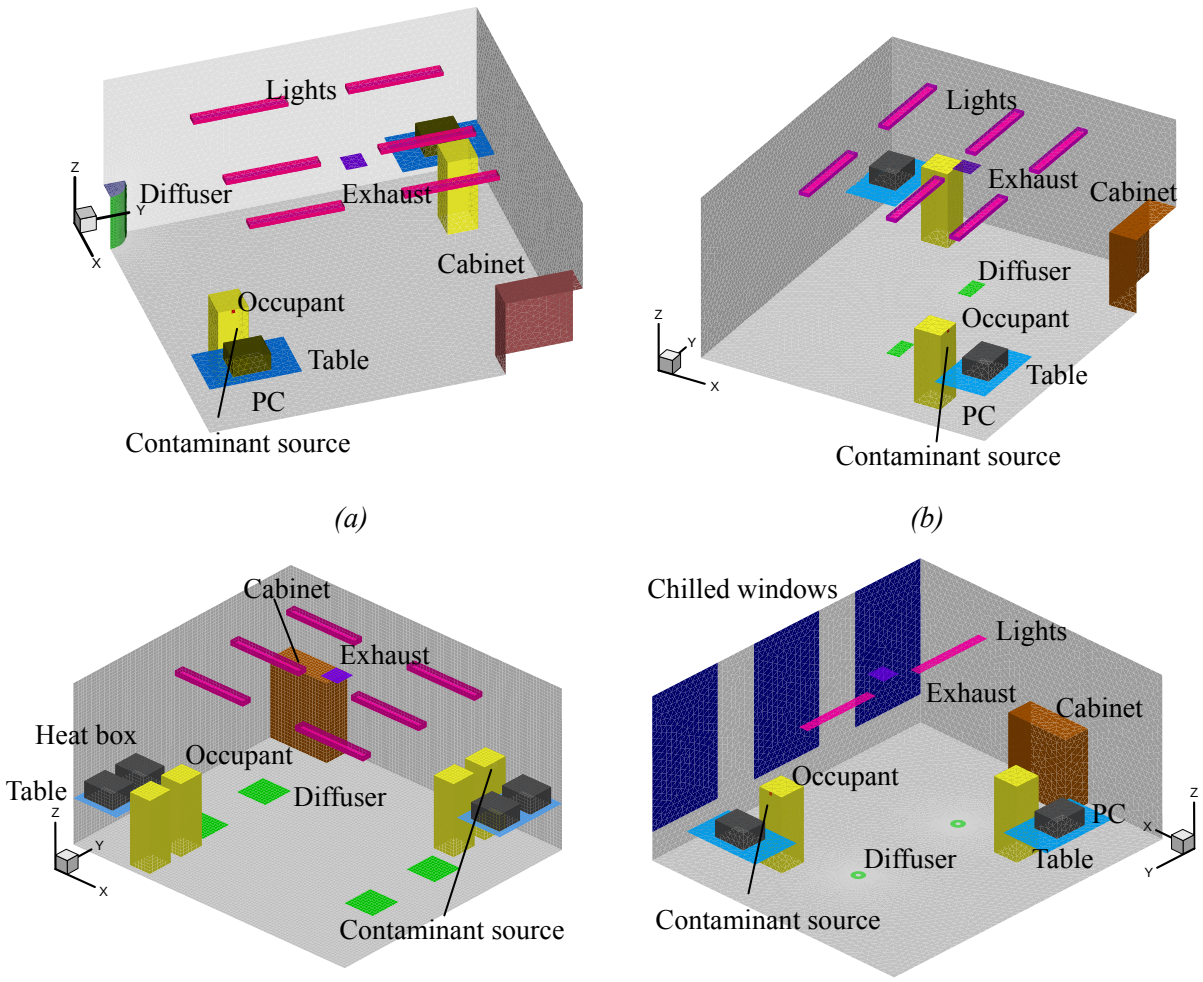

Fig. 3. Layouts of four displacement ventilation cases with (a) a corner-mounted, quarter-circular perforated diffuser; (b) two floor-grille diffusers; (c) four floor-perforated-panel diffusers; or (d) two floor-swirl diffusers.

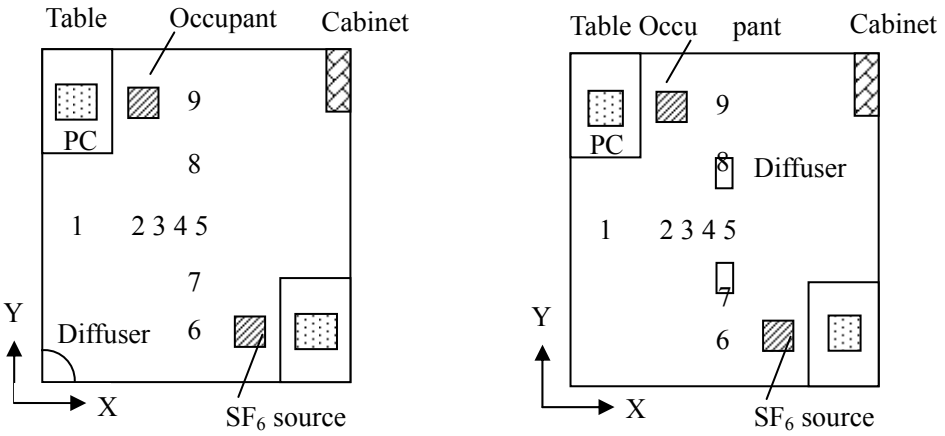

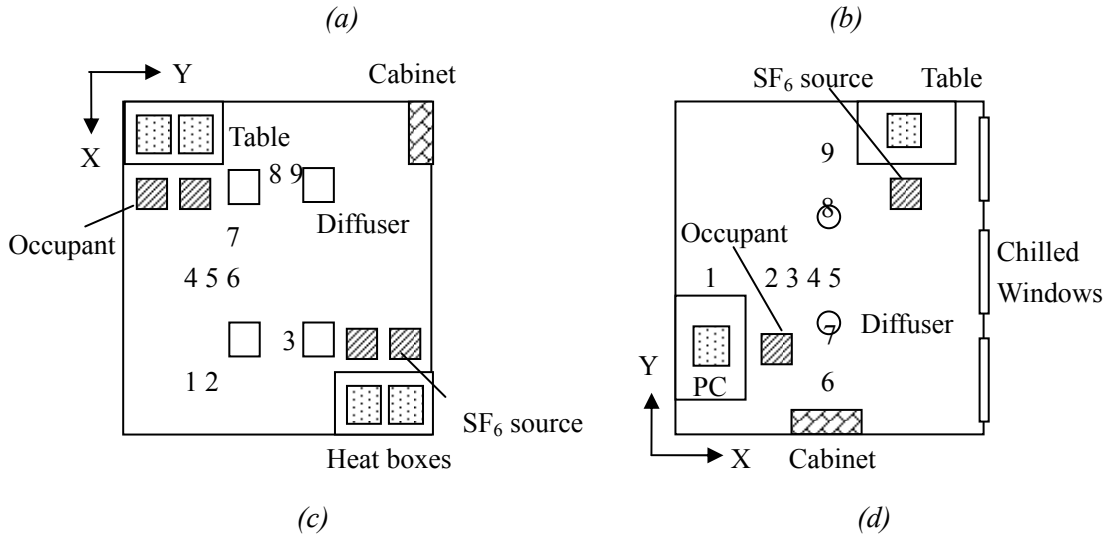

Fig. 4.Top view of the nine experimental measurement locations for the four displacement ventilation cases with (a) a corner-mounted, quarter-circular perforated diffuser; (b) two floor-grille diffusers; (c) four floor-perforated-panel diffusers; or (d) two floor-swirl diffusers.

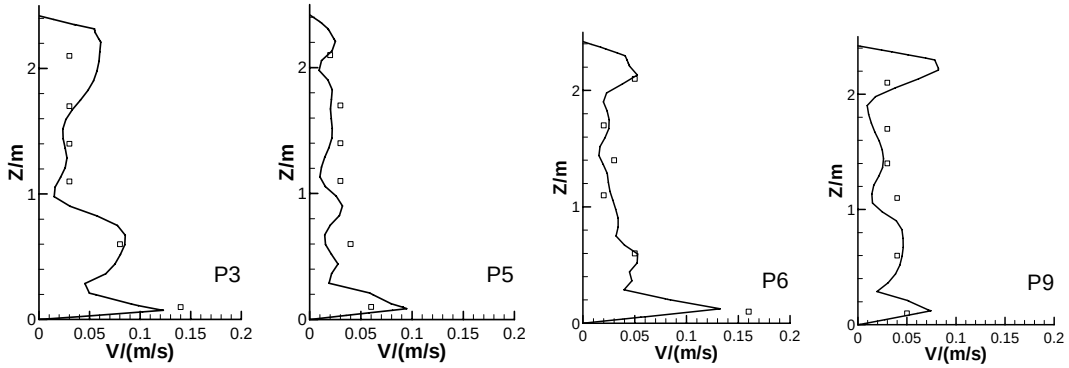

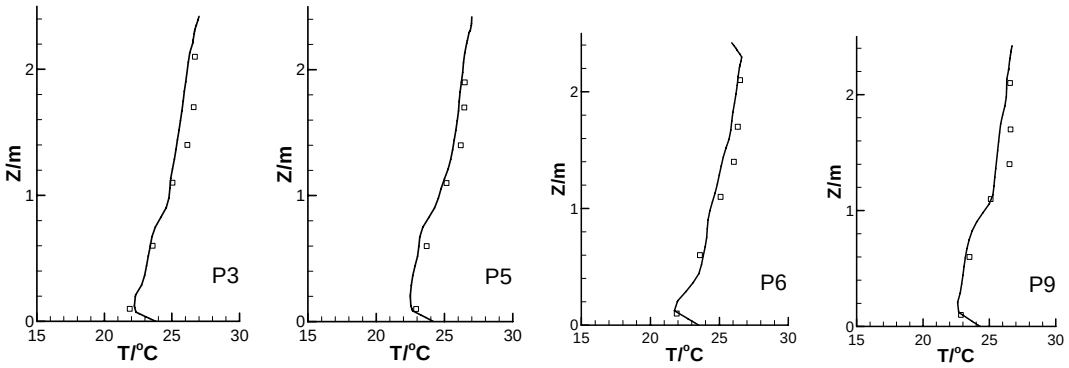

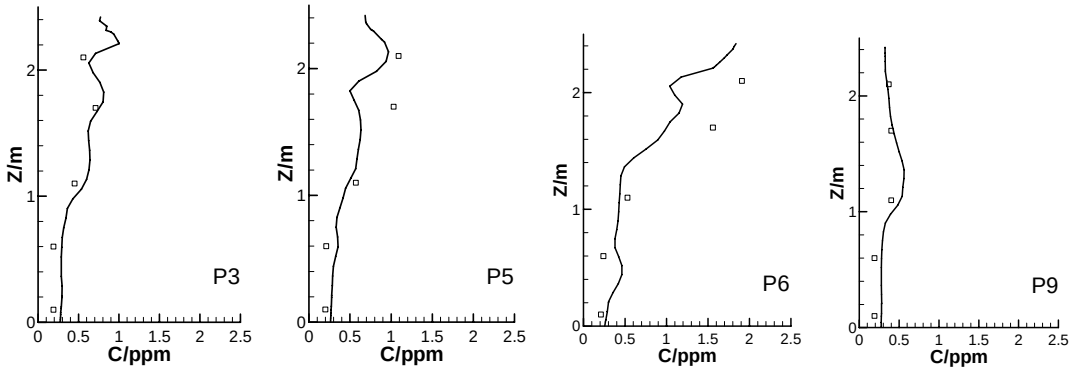

(c)

Fig. 5. Comparison of the vertical profiles in four representative locations by CFD and by experiment for the office with the quarter-circular-perforated diffuser, lines for CFD and symbols for experiment: (a) air velocity; (b) air temperature; and (c) SF_6 concentration.

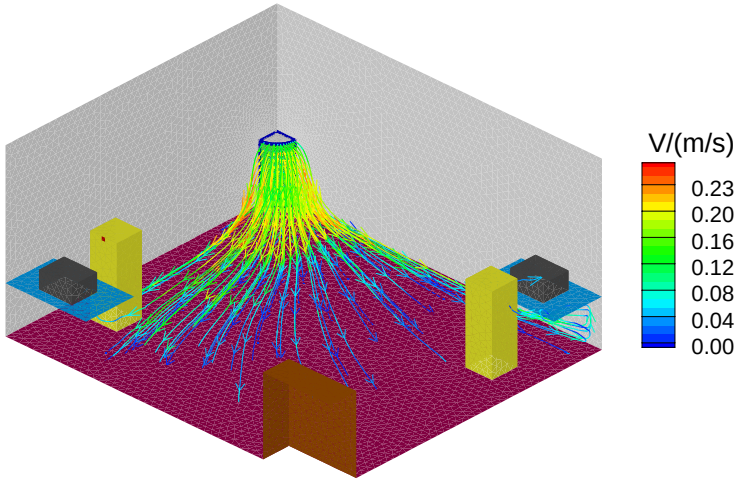

Fig. 6. Flow path lines from the quarter-circular-perforated diffuser.

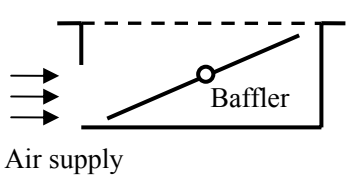

0.44 1.2	4 1.0	6
0.35 0.2	2 0.3	5
0.22	0.22 0.2	2

X

Y

(a) *(b)*

Fig. 7. (a) A sectional view of the inside structure of the grille diffuser and (b) the measured velocity on the diffuser surface (m/s).

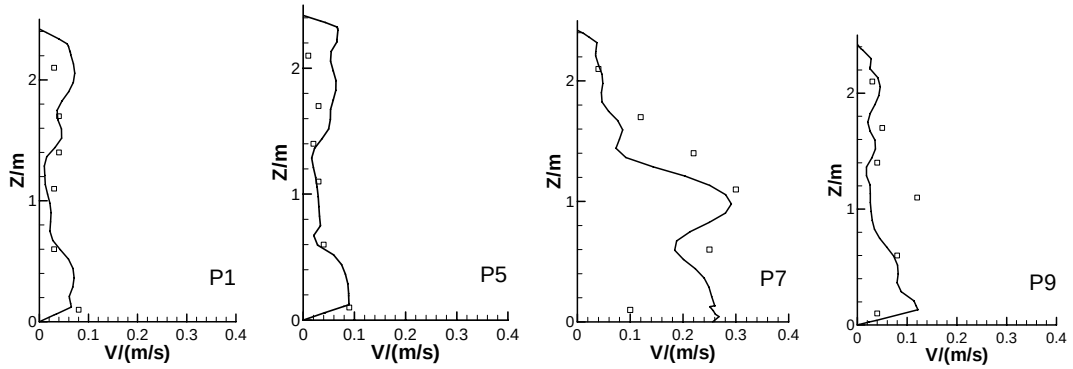

(a)

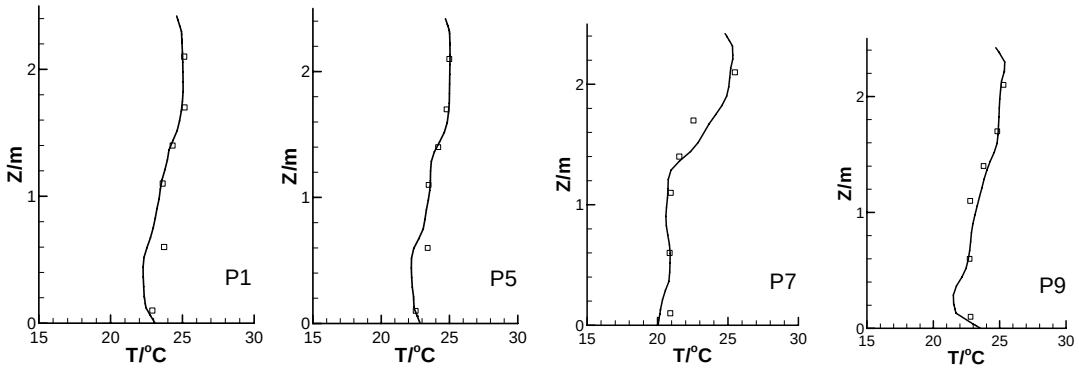

(b)

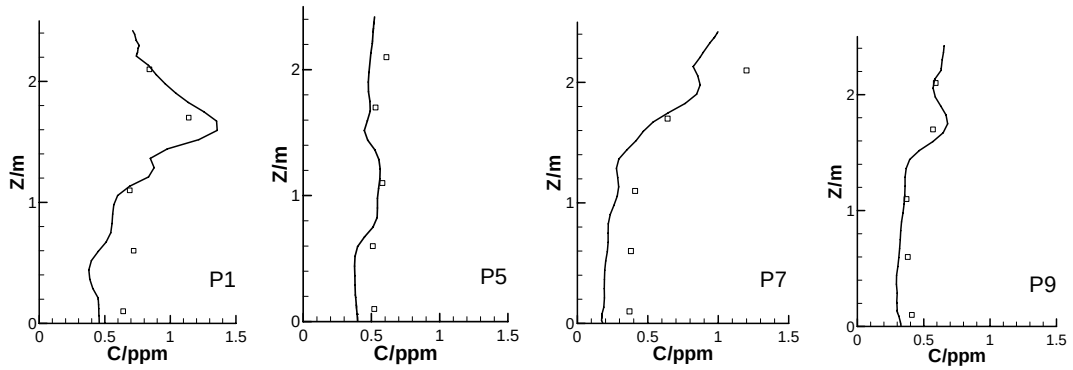

(c)

Fig. 8. Comparison of the vertical profiles in four representative locations by CFD and by experiment for the office with the two grille diffusers, lines for CFD and symbols for experiment: (a) air velocity; (b) air temperature; and (c) SF_6 concentration.

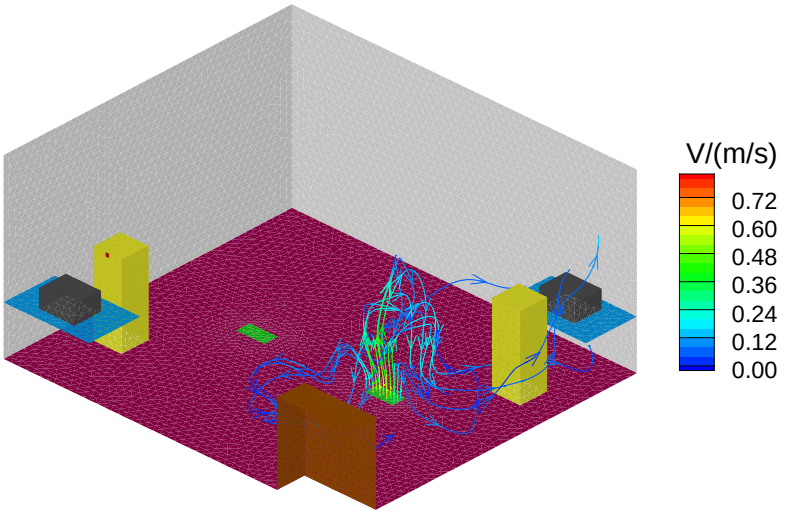

Fig. 9. Flow path lines from the grille diffuser.

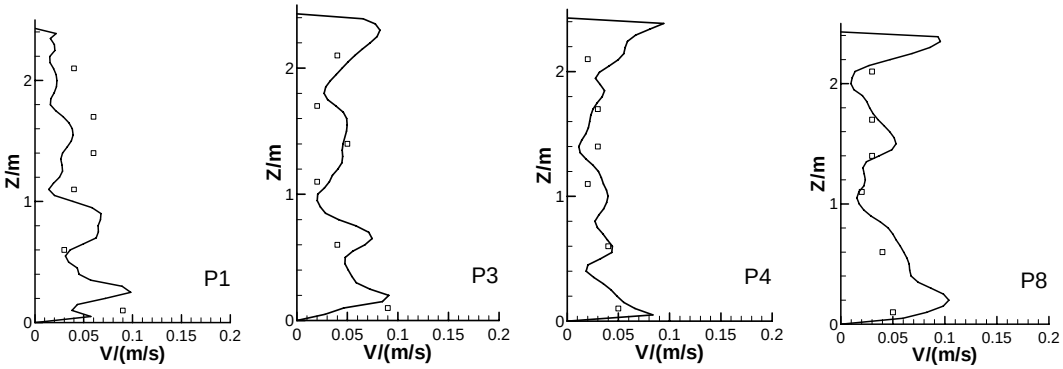

(a)

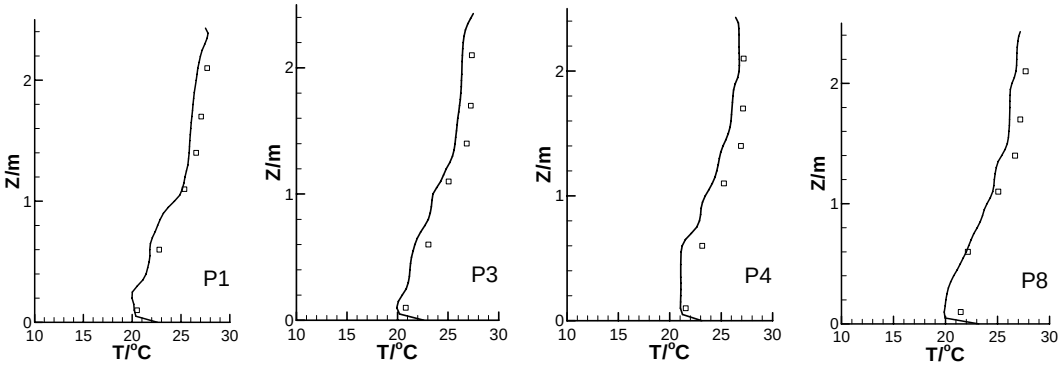

(b)

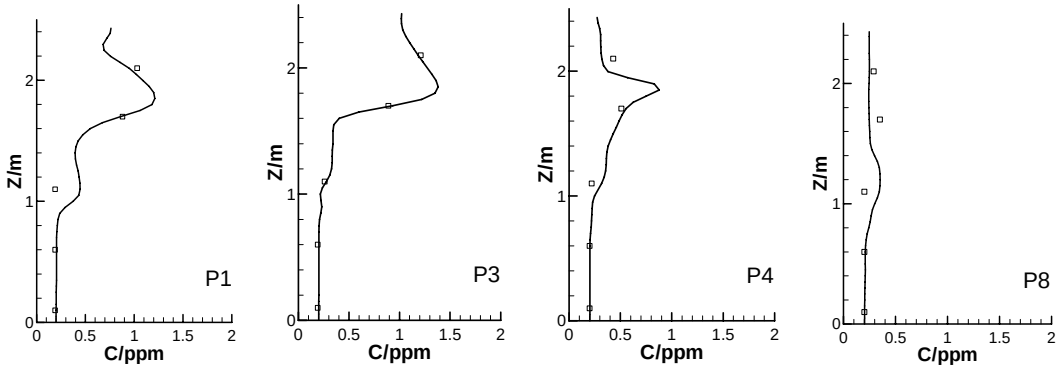

(c)

Fig. 10. Comparison of the vertical profiles in four representative locations by CFD and by experiment for the workshop with the four floor-perforated-panel diffusers, lines for CFD and symbols for experiment: (a) air velocity; (b) air temperature; and (c) SF_6 concentration.

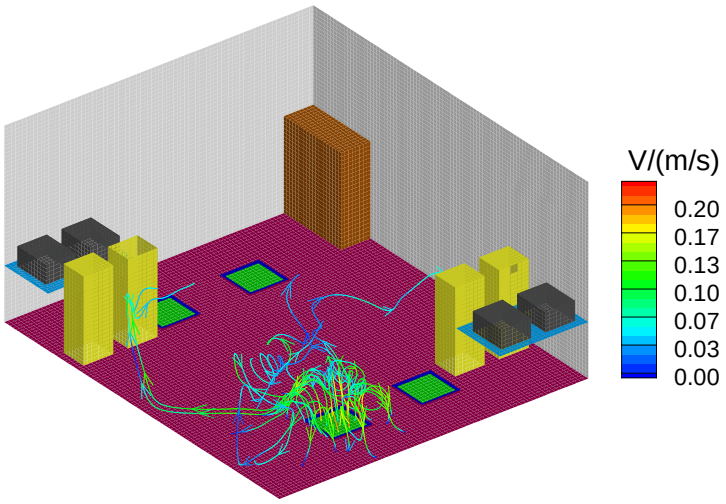

Fig. 11. Flow path lines from the perforated panel diffuser

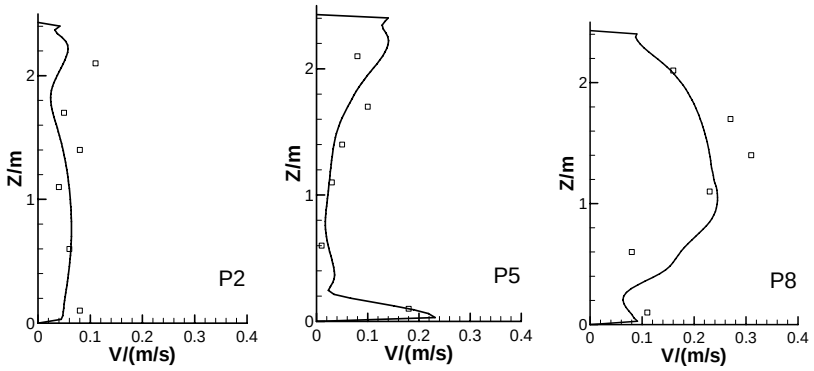

(a)

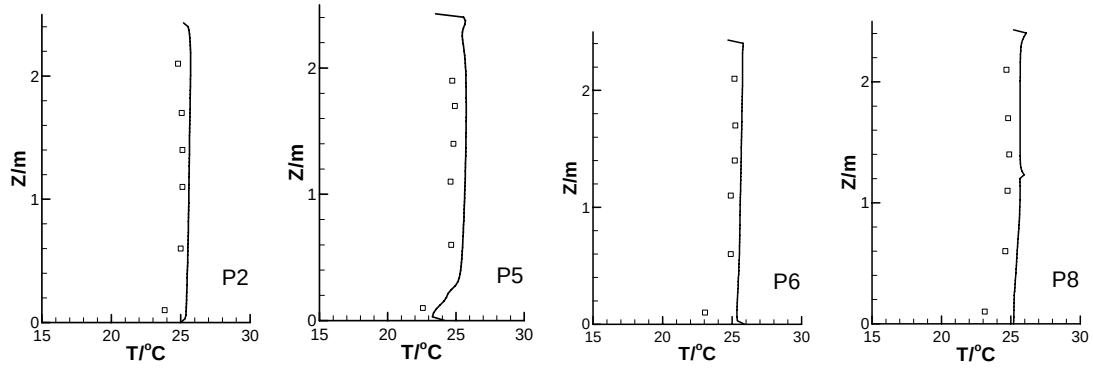

(b)

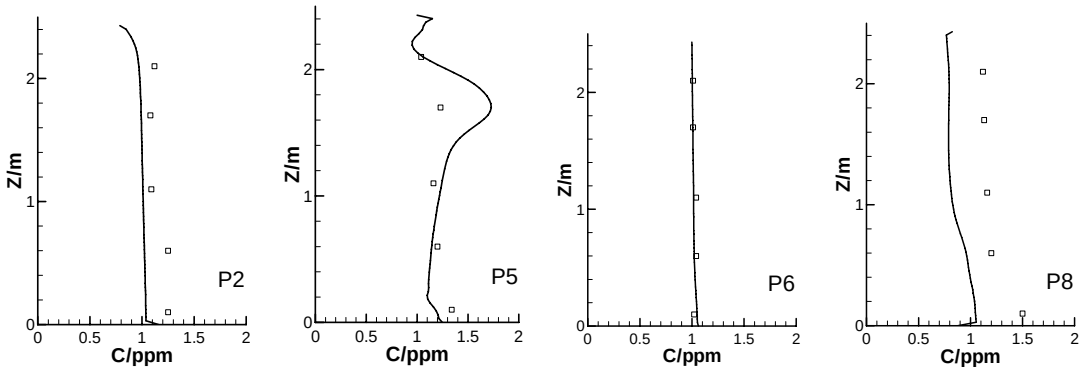

(c)

Fig. 12. Comparison of the vertical profiles in four representative locations by CFD and by experiment for the office with the two swirl diffusers, lines for CFD and symbols for experiment: (a) air velocity; (b) air temperature; and (c) SF_6 concentration.

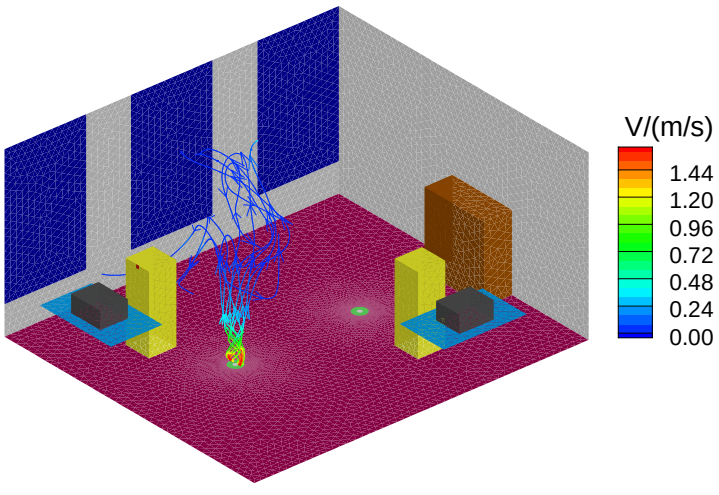

Fig. 13. Flow path lines from the swirl diffuser under heating condition